A PROCEDURE TO DETERMINE THE INTRINSIC MODEL OF CNTFETs FOR RF APPLICATIONS

Roberto Marani & Anna Gina Perri[1]
Electrical and Information Engineering Department, Polytechnic University of Bari, Italy

ABSTRACT

The aim of this paper is to present a procedure to determine the intrinsic model of Carbon NanoTube Field Effect Transistors (CNTFETs) for RF applications. In particular an active model, deduced from S parameters measurements, already proposed by us, is examined. Moreover, through a de-embedding procedure, which allows to remove random errors in measured S parameters of small-signal device, we evaluate the intrinsic model of CNTFETs to implement directly in simulation software.

Keywords: *Nanoelectronic Devices, CNTFETs, Modelling, RF Characterization.*

1. INTRODUCTION

One of the main differences between Si based VLSI and RF electronics is the choice of semiconductor materials and transistor types. While Si is the only semiconductor used in VLSI, a wide range of alternative materials and devices are present in RF electronics.

CNTFETs (Carbon Nanotube Field Effect Transistors) are novel devices that are expected to sustain the transistor scalability while increasing its performance. One of the major differences between CNTFETs and MOSFETs is that the channel of the devices is formed by Carbon NanoTubes (CNTs) instead of silicon, which enables a higher drive current density, due to the larger current carrier mobility in CNTs compared to bulk silicon [1]. In particular, with CNTs we obtain good operation even at very high frequencies [2-8].

A number of different geometries and solutions for CNTFETs, as well as their DC and low frequency behavior [9], have been evaluated and reported in many papers. By contrast, radio frequency (RF) operation has not been so deeply analyzed yet [10].

As it is known, RF systems critically depend on their front-end circuit blocks, such as power amplifier, low-noise amplifier and so on.. These circuits are typically designed using simulators with compact models representing the devices on a chip. The requirements for device models used for RF design are quite stringent since they need to describe a typically nonlinear device accurately over a wide range of bias, frequency and temperature [11]. Moreover, in order to have low simulation time, it is necessary to simply the device behaviour introducing lumped element two-port network models.

In this paper we present a de-embedding procedure, applicable to any CNTFET structures, in order to determine the intrinsic model of CNTFETs for RF applications, to implement directly in simulation software.

The presentation of the paper is organized as follows. In Section 2 we briefly summarize the main characteristics of CNTs, while in Section 3 we examine the technological and electrical characteristics of CNTFET analyzed. In Section 4 a description of the our RF model is presented. The de-embedding procedure is in detail analyzed in Section 5, togheter with the discussion of relative results. The conclusions are described in Section 6.

2. REVIEW OF CNTs

A Carbon Nanotube, discovered in 1991 by S. Iijima, is a sheet of hexagonal arranged carbon atoms rolled up in a tube of a few nanometers in diameter, which can be many microns long. Graphene is a single sheet of carbon atoms arranged in the well known honeycomb structure [1] [12]. This lattice is shown in Fig. 1.

Carbon has four valence electrons, three of which are used for the sp^2 bonds. In sp^2-hybridization an electron is promoted from the 2*s*-orbital to a *p*-orbital, and then two electrons from different 2*p*-orbitals combine with the single electron left in the 2*s*-orbital to generate three equivalent sp^2-orbitals. These orbitals are planar with 120^o between the major lobes, and the remaining *p*-orbital is perpendicular to this plane. The leftover *p*-orbital is perpendicular to the graphene, and electrons in this orbital bond to other carbon atoms through weak π-bonds. The electrons in the *p*-orbitals are thus loosely bound and responsible for the conductance of graphite. Since the CNT is

[1] Address correspondence to this author at Dipartimento di Ingegneria Elettrica e dell'Informazione, Laboratorio di Dispositivi Elettronici, Politecnico di Bari, Italy; Phone: +39-80-5963314/5963427; Fax: +39-80-5963410; E-mail: annagina.perri@poliba.it

made up of one or more sheets of graphene rolled up in a tubular structure, the binding in the CNT is nearly identical to that of graphite. The differences in binding are due to the larger inter-shell distance in CNT compared to the interlayer distance of graphite, and the curvature of the graphene sheets [13-15].
Fig. 1 shows the construction of a graphene sheet.

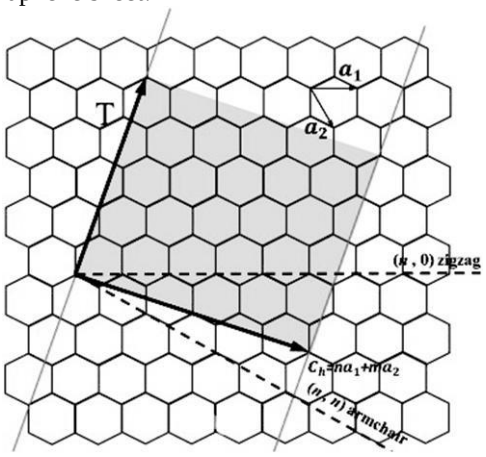

Figure 1. Lattice of graphene. Carbon atoms are located at each crossings and the lines indicate the chemical bonds, which are derived from sp^2-orbitals. C_h is chiral vector, T is tube axis; θ is chiral angle [1].

The chiral vector, C_h, is the vector perpendicular to tube axis T, which is given by:

$C_h = n\bar{a}_1 + m\bar{a}_2$
(1)

being n and m a pair of integers and $\bar{a}_1$ and $\bar{a}_2$ the lattice vectors, which can be written as:

$$\bar{a}_1 = \left(\frac{\sqrt{3}}{2}a_0, \frac{3a_0}{2}\right) \qquad \bar{a}_2 = \left(-\frac{\sqrt{3}}{2}a_0, \frac{3a_0}{2}\right) \tag{2}$$

where a_0 is the iner-atomic distance between each carbon atom and its neighbor, equal to 1.42 Å.
The p_z atomic-orbitals are oriented perpendicular to the plane and are rotational symmetric around the z-axis.
A CNT can be multi-wall (MWCNT) or single-wall (SWCNT) [1]. A MWCNT (Fig. 2) is composed of more than one cylinder whereas a SWCNT (Fig. 3) is a single cylinder.

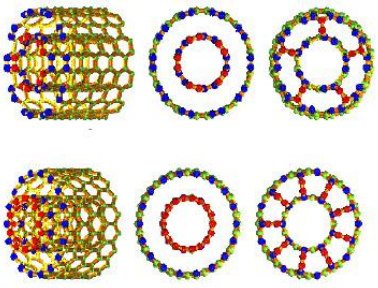

Figure 2. Structure of a MWCNT.

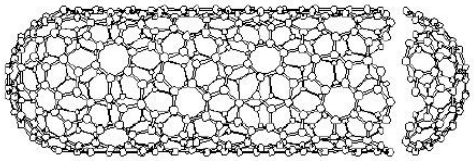

Figure 3. Structure of a SWCNT.

Depending on their chiral vector, CNTs have either semi-conducting or metallic behaviour.
In particular, if n = m or n – m = 3i, where i is an integer, the nanotube is metallic; in other cases it shows semi-conducting property [1] [12].
The diameter of the CNT can be calculated by the following equation:

$$d = \left|\frac{C_h}{\pi}\right| = \frac{a_0}{\pi}\sqrt{n^2 + m^2 + nm} \tag{3}$$

The chiral angle shows the chirality of nanotube and can be found by the following equation.

$$\cos\varphi = \frac{(n+m)\sqrt{3}}{2\sqrt{n^2+m^2+nm}} \quad (4)$$

If (n = m, φ = 0°), CNTs are defined as armchair-type, while, if (m = 0, φ = 30°), as zig-zag type.
Fig. 4 shows the conduction band and valence band energy level diagram of carbon nanotube [16].

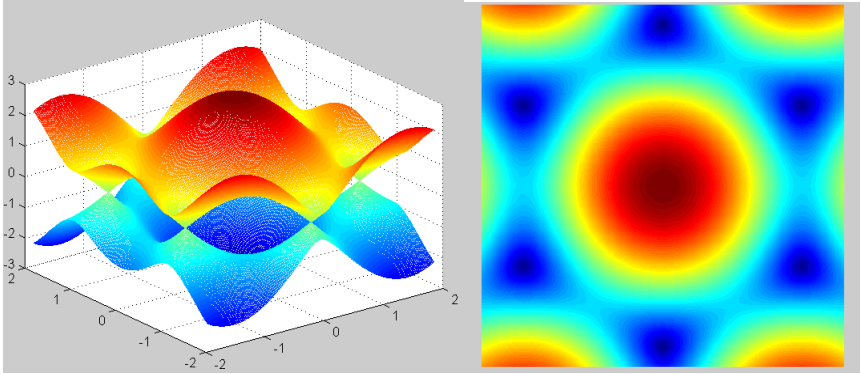

Figure 4. Energy level diagram of carbon nanotube.

In particular, for a SWCNT having a semiconductor behaviour, the band gap E_{gap} is expressed by the following relation [1]:

$$E_{gap} = \frac{2\gamma_0 a_0}{d} \quad (5)$$

where γ_0 is the carbon-to-carbon tight-binding overlap energy.
A straightforward application of this semiconducting property of CNTs is to form a field-effect transistor (FET) analogous to the MOSFET [1].
Carbon NanoTube Field Effect Transistors (CNTFETs), in fact, are FETs using a carbon nanotube as channel, and are regarded as an important contending device to replace conventional silicon transistors [17].

3. TECNOLOGICAL AND ELECTRICAL CHARACTERISTICS OF CNTFET ANALYZED

In this paper we have considered the device proposed in [18-19]. It was a *back-gate* CNTFET, fabricated on a n^{++} substrate. The gate oxide layer was realized by thermal deposition, then carbon nanotubes were grown in order to form the channel, using CVD (*Chemical Vapor Deposition*). Finally, a Ti/Au bilayer was patterned to form metal electrodes. In that way, mainly single-walled CNTs were obtained; a high source-drain voltage was applied to break most of the metallic nanotubes, without affecting semiconducting ones. A SEM photo of the structure is shown in Fig. 5, in which the insert indicates the cross section of the employed back-gate geometry.

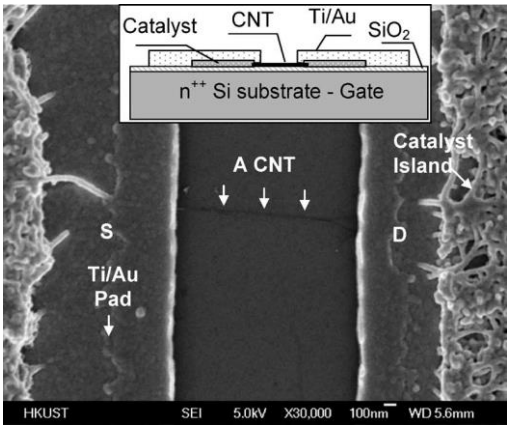

Figure 5. SEM photo of the analyzed CNTFET structure (from [19]).

The I_{DS}-V_{DS} output characteristics for different gate-source voltage values (V_{GS}) are shown in Fig. 6.

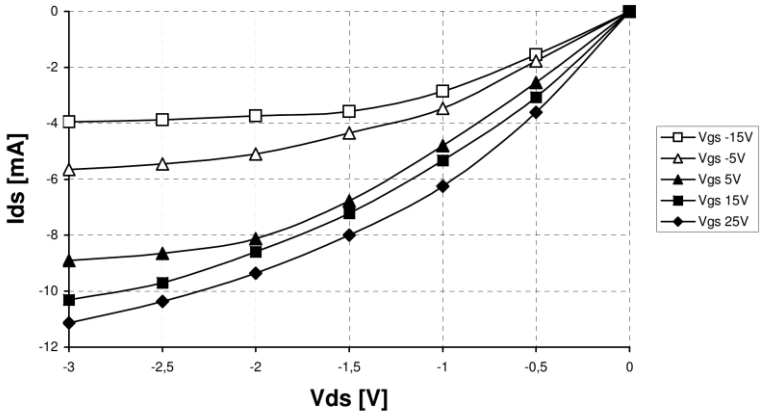

Figure 6. I_{DS} -V_{DS} characteristics for different V_{GS} values.

Despite the fact presence of some metallic CNTs the device operates similarly to a typical field-effect transistor, showing its *ambipolar* behavior, i.e. the channel is formed for either positive or negative V_{GS} values, even if it shows much better performances when it is biased like a p-channel FET (negative V_{GS}).
S parameters measurements, from very low frequency up to 12 GHz, were performed employing a HP 8510 network analyzer [20], where the bias values of the examined CNTFET are V_{DS} = - 3 V and V_{GS} = -15 V.
Provided that the measurements aimed at mainly analyzing transmission properties of the CNT-based channel, rather than amplification performances, a very high V_{GS} was chosen. In this situation the trans-conductance is low (80 □S), because a variation in V_{GS} corresponds to an almost negligible change in V_{DS}, so that the transistor works substantially as a passive device.
S_{11} and S_{21} parameters, both in magnitude and phase, were measured for several frequencies.
However they are affected by parasitic effects due to the measurements setup.
Therefore, in order to extract some information on CNTFET intrinsic behaviour, a de-embedding procedure has to be performed, as we will explain in Section 5.

4. OUR RF CNTFET MODEL

In [21] we have presented a new active model, shown in Fig. 7, whose parameters values have been obtained through a best- fitting procedure between the measured and simulated S parameters.
In particular the proposed model is an active, non symmetrical circuit, since it takes into account the transistor trans-conductance g_m, whose values, deduced from Fig. 6, are reported in Fig. 8.
Similarly, in Fig.9 we have reported the output impedance of transistor deduced from I-V characteristics.

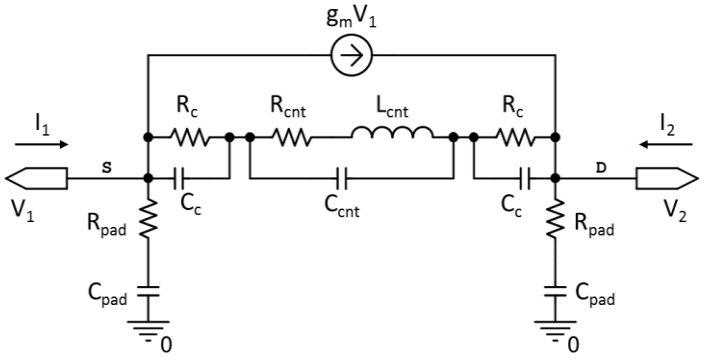

Figure 7. The proposed RF CNTFET model.

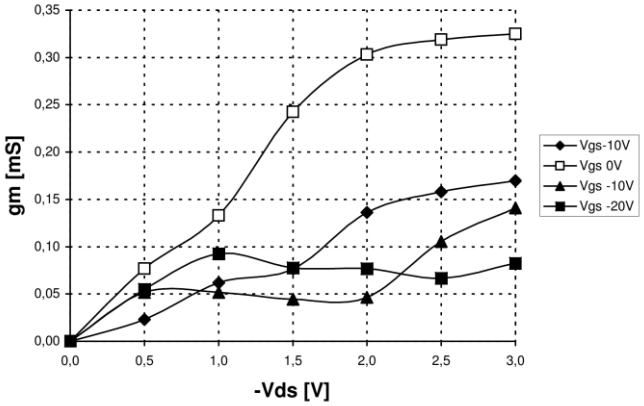

Figure 8. CNTFET trans-conductance g_m versus V_{DS} for different V_{GS} values.

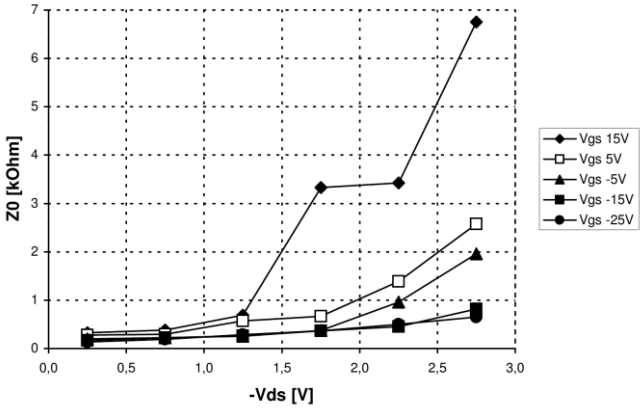

Figure 9. CNTFET Z_0 versus V_{DS} for different V_{GS} values.

The element, indicated with R_{pad} and C_{pad}, model the parasitic effects due to measurement setup (metal pads). Source and drain contacts between the channel and pads are considered both resistive (R_c) and capacitive (C_c).
Finally, we have modeled the transmission properties of the channel by the $R_{CNT} - L_{CNT}$ series, in parallel with C_{CNT} source-drain capacitance.
Moreover initial simulations have brought us to omit source-substrate and drain-substrate capacitances, as well as the DC conductance of few possible metallic CNTs in the channel, since their effects are negligible.
Definitely the unknown circuital elements of model of Fig. 7 are: R_{CNT}, L_{CNT}, C_{CNT}, R_c, C_c, R_{pad}, and C_{pad}.
In order to determine their values, we have performed a *best fitting procedure*, based on the minimization of an objective function, formed by the values of the squared differences between the measured and calculated values of S_{11} and S_{21} parameters [21]. In Table 1we have reported the circuit parameters values, obtained through the best fitting procedure, previously illustrated.

Element	Calculated value
R_{CNT}	3.33 kΩ
L_{CNT}	149 nH
C_{CNT}	0.542 pF
R_c	40.3 Ω
C_c	≈ 0 F
R_{pad}	1.39 Ω
C_{pad}	4.46 pF

Table I. Circuital values of our model.

However the measured S parameters are affected by random errors and therefore it is necessary to use a e de-embedding procedure that removes existing errors in measured S-parameters of high-impedance devices.

5. DE-EMBEDDING PROCEDURE

In our model of Fig. 6 parasitic effects due to the measurement setup have been modeled by the two R_{pad} - C_{pad} branches; whose values have been determined by the fitting procedure, previously illustrated.
Eliminating the two branches, we have extracted. a network, which theoretically models the intrinsic device. In this way the S parameter results have been de-embedded by the effects of metal pads.
In Fig. 10 and Fig. 11 we have reported S_{11} and S_{21} parameters, both in magnitude and phase, measured and modeled for several frequencies, respectively, after de-embedding.

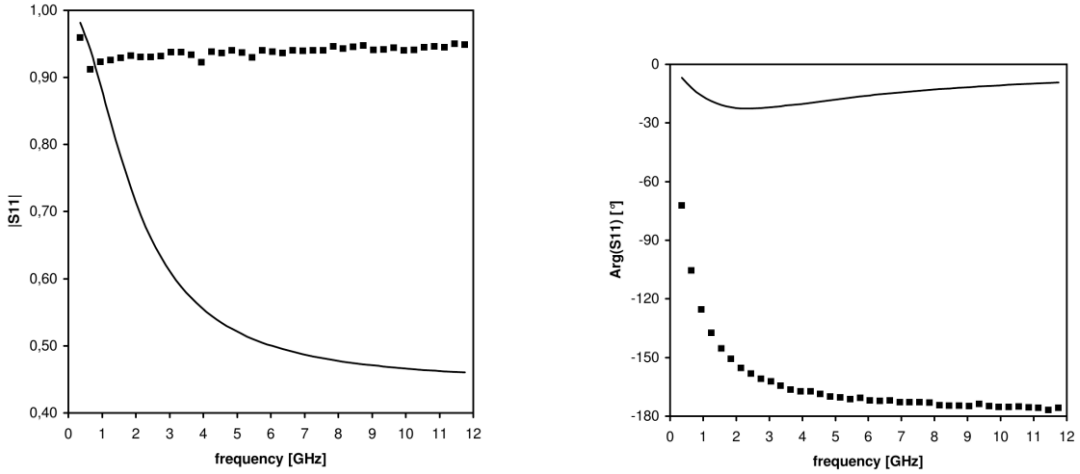

(a) (b)

Figure 10. Comparison between measured (■) and fitted (continuous line) of S_{11}, in magnitude (a) and phase (b) after de-embedding.

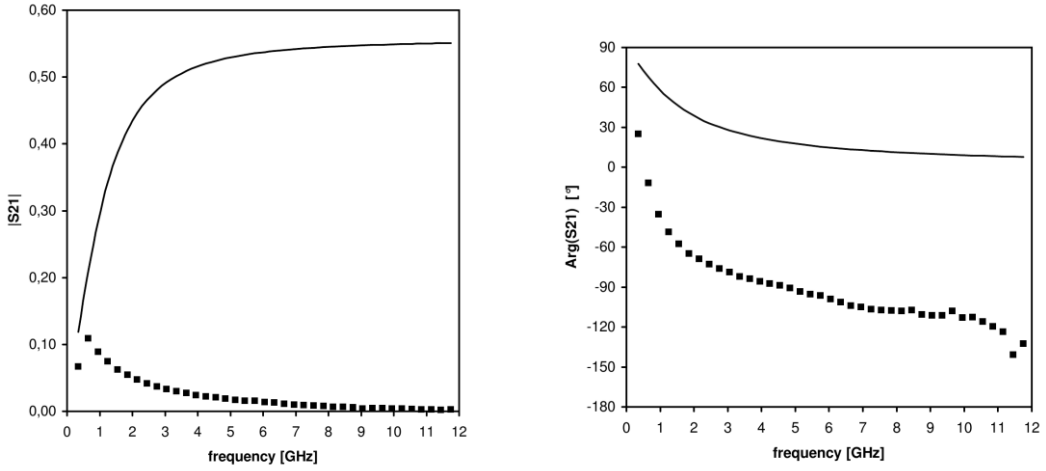

(a) (b)

Figure 11. Comparison between measured (■) and fitted (continuous line) of S_{21}, in magnitude (a) and phase (b) after de-embedding.

From the analysis of Fig. 10 and Fig. 11 we have confirmed that CNTFET presents a good behaviour at higher frequencies, while the strong de-embedding correction shows the main importance of the technology used to realize the device, which limits the CNTFET properties.

6. CONCLUSIONS

We have proposed a de-embedding procedure, applicable to any CNTFET structures, in order to determine the intrinsic RF model of CNTFETs, whose circuital elements have been deduced from S parameters measurements up to 12 GHz, through a best fitting between the measured and calculated values of S_{11} and S_{21} parameters.

The proposed de-embedding procedure allows us to remove random errors in measured S parameters of small-signal device, obtaining the intrinsic model to implement directly in simulation software for electronic circuits CAD.

7. REFERENCES

[1] A. G. Perri: Dispositivi Elettronici Avanzati, Progedit Editor, Bari, Italy; ISBN: 978-88-6194-081-9, (2011).

[2] R. Marani, A.G. Perri: A Compact, Semi-empirical Model of Carbon Nanotube Field Effect Transistors oriented to Simulation Software, *Current Nanoscience*, **7**(2), 245-253, (2011).

[3] G. Gelao, R. Marani, R. Diana, A.G. Perri: A Semi-Empirical SPICE Model for n-type Conventional CNTFETs, *IEEE Transactions on Nanotechnology*, **10**(3), 506-512, (2011).

[4] R. Marani, A.G. Perri: Simulation of CNTFET Digital Circuits: a Verilog-A Implementation, *International Journal of Research and Reviews in Applied Sciences*, **11**(1), 74-81, (2012).

[5] R. Marani, A.G. Perri: Modelling and Implementation of Subthreshold Currents in Schottky Barrier CNTFETs for Digital Applications, *International Journal of Research and Reviews in Applied Sciences*, **11**(3), 377-385, (2012).

[6] R. Marani, G. Gelao, A.G. Perri: Comparison of ABM SPICE library with Verilog-A for Compact CNTFET model implementation, *Current Nanoscience*, **8**(4), 556-565, (2012).

[7] R. Marani, G. Gelao, A.G. Perri: Modelling of Carbon Nanotube Field Effect Transistors oriented to SPICE software for A/D circuit design, *Microelectronics Journal*, DOI:10.1016/j.mejo.2011.07.012, 33-39, (2013).

[8] F.R. Madriz, J.R. Jameson, S. Krishnan, X. Sun, C.Y. Yang: Circuit Modeling of High-Frequency Electrical Conduction in Carbon Nanofibers. *IEEE Transactions on Electron Devices*, **56**(8), 1557- 1561, (2009).

[9] R. Marani, A.G. Perri: A DC Model of Carbon Nanotube Field Effect Transistor for CAD Applications. *International Journal of Electronics*, **99**(3), 427 – 444, (2012).

[10] J.-M. Bethoux, H. Happy, A. Siligaris, G. Dambrine, B. J. V. Derycke,.J.P. Bourgoin: Active properties of carbon nanotube field-effect transistors deduced from S parameters measurements, *IEEE Transactions on Nanotechnology*, **5**(4), 335-342, (2006).

[11] M. Schröter, M. Haferlach, A. Pacheco-Sanchez, S. Mothes, P. Sakalas, M. Claus: A Semiphysical Large-Signal Compact Carbon Nanotube FET Model for Analog RF Applications, *IEEE Transactions on Electron Devices*, **62**(1), 52-60, (2015).

[12] A. G. Perri: Modelling and Simulations in Electronic and Optoelectronic Engineering. Editor Research Signpost, Kerata, India, ISBN: 978-81-308-0450-7, (2011).

[13] A. K. Geim, K. S. Novoselov: The rise of graphene. *Nature Mater.* **6,** 183–191 (2007).

[14] M. Y. Han, B. Őzyilmaz, Y. Zhang, P. Kim,: Energy band gap engineering of grapheme nanoribbons. *Phys. Rev. Letters* **98,** 206805 (2007).

[15] Y. W. Son, M. L. Cohen, S. G. Louie: Energy gaps in graphene nanoribbons. *Phys. Rev. Letters* **97,** 216803 (2006).

[16] R. Marani, A.G. Perri: A Light Model to Evaluate the Dispersion Equation of Carbon Nanotubes, *International Journal of Research and Reviews in Applied Sciences*, **15**(1), 57-61, (2013).

[17] Ph. Avouris, M. Radosavljević, S.J. Wind, Carbon Nanotube Electronics and Optoelectronics, in Applied Physics of Carbon Nanotubes: Fundamentals of Theory, Optics and Transport Devices, Springer-Verlag, Berlin, Germany, ISBN: 978-3-540-23110-3, (2005).

[18] X. Huo, M. Zhang, P. C. H. L. Q. Chan, Z. K. Tang: High Frequency S parameters Characterization of Back-gate Carbon Nanotube Field-Effect Transistors. *Proceedings of International Electron Devices Meeting*, IEDM Technical Digest, (2004).

[19] M. Zhang, X. Huo, P. C. H. L. Q Chan, Z. K. Tang: Radio-Frequency Transmission Properties of Carbon Nanotubes in a Field-Effect Transistor Configuration. *Electron Device Letters*, 668-670, (2006).

[20] Agilent Technologies. Agilent 8510 Network Analyzer, (2006).

[21] G. Gelao, R. Marani, P. Soldano, A.G. Perri: An Active CNTFET Model for RF Characterization Deduced from S Parameters Measurements, *Current Nanoscience*, **11**(1), 36-40, (2015).